

Modulating quantum transport by transient chaos

Rui Yang, Liang Huang, Ying-Cheng Lai, and Louis M. Pecora

Citation: *Appl. Phys. Lett.* **100**, 093105 (2012); doi: 10.1063/1.3690046

View online: <http://dx.doi.org/10.1063/1.3690046>

View Table of Contents: <http://apl.aip.org/resource/1/APPLAB/v100/i9>

Published by the [American Institute of Physics](#).

Related Articles

Spin accumulation in parallel-coupled quantum dots driven by a symmetric dipolar spin battery
J. Appl. Phys. **111**, 053708 (2012)

Forming delocalized intermediate states with realistic quantum dots
J. Appl. Phys. **111**, 056102 (2012)

Spin-bias modulated Kondo effect in an interacting quantum dot
J. Appl. Phys. **111**, 07C309 (2012)

A statistical exploration of multiple exciton generation in silicon quantum dots and optoelectronic application
Appl. Phys. Lett. **100**, 071111 (2012)

Effect of a lateral electric field on an off-center single dopant confined in a thin quantum disk
J. Appl. Phys. **111**, 034317 (2012)

Additional information on *Appl. Phys. Lett.*

Journal Homepage: <http://apl.aip.org/>

Journal Information: http://apl.aip.org/about/about_the_journal

Top downloads: http://apl.aip.org/features/most_downloaded

Information for Authors: <http://apl.aip.org/authors>

ADVERTISEMENT

NEW!

iPeerReview

AIP's Newest App



Authors...
Reviewers...

Check the status of
submitted papers remotely!

AIP | Publishing

Modulating quantum transport by transient chaos

Rui Yang,¹ Liang Huang,^{1,2,a)} Ying-Cheng Lai,^{1,3} and Louis M. Pecora⁴

¹*School of Electrical, Computer, and Energy Engineering, Arizona State University, Tempe, Arizona 85287, USA*

²*Institute of Computational Physics and Complex Systems, and Key Laboratory for Magnetism and Magnetic Materials of MOE, Lanzhou University, Lanzhou, Gansu 730000, China*

³*Department of Physics, Arizona State University, Tempe, Arizona 85287, USA*

⁴*Materials Physics and Sensors, U.S. Naval Research Laboratory, Washington, DC 20375, USA*

(Received 7 October 2011; accepted 9 February 2012; published online 29 February 2012)

We propose a scheme to modulate quantum transport in nanostructures based on classical chaos. By applying external gate voltage to generate a classically forbidden region, transient chaos can be generated, and the escape rate associated with the underlying non-attracting chaotic set can be varied continuously by adjusting the gate voltage. We demonstrate that this can effectively modulate the quantum conductance-fluctuation patterns. A theory based on self-energies and the spectrum of the generalized non-Hermitian Hamiltonian of the open quantum system is developed to understand the modulation mechanism. © 2012 American Institute of Physics. [<http://dx.doi.org/10.1063/1.3690046>]

When electrons pass through a nanostructure, the conductances can depend sensitively on electronic and system parameters.¹ For example, as the Fermi energy of the conducting electron changes, the conductance can exhibit strong fluctuations.² Conceivably, there are applications in nanoscience and nanotechnology where severe conductance fluctuations are to be eliminated to achieve stable device operation. An outstanding question is then: Can practical and experimentally feasible schemes be devised to modulate the quantum conductance fluctuations? The purpose of this letter is to propose, demonstrate, and understand that classical *transient chaos* can be used to effectively modulate quantum transport. While previous works elucidated the basic physics underlying the effect of chaos on quantum transport,² our proposed scheme can be implemented experimentally to systematically modulate quantum transport dynamics. As will be shown, our proposed scheme of a Sinai-type of open billiard quantum dot, where the size of the central circular region can be experimentally modulated in a systematic manner, is one such design. We will demonstrate computationally for both non-relativistic two-dimensional electron gas (2DEG) and relativistic (graphene³) quantum-dot (QD) systems that when the radius of the central potential region is varied so that the characteristics of the corresponding chaotic dynamics are modified, the quantum conductance-fluctuation patterns are effectively modulated. To our knowledge, although controlling chaos⁴ has been studied for more than two decades, prior to our work there were no reports on exploiting chaos for systematic control/modulation of quantum transport.⁵ We will develop a physical theory based on the complex spectrum of the device Hamiltonian, which is non-Hermitian, to understand the modulation mechanism.

Intuitively, why classical chaos can be exploited to modulate quantum transport can be argued as follows. Sharp conductance fluctuations are typically caused by quantum pointer states, which are resonant states of finite but long life-

time formed inside the nanostructure.⁶ For example, for a closed quantum-dot system whose classical dynamics is regular or contains a significantly regular component, there are stable periodic orbits in the classical limit. When leads are attached to the QD, some periodic orbits can still survive, leading to quantum pointer states. As a result, narrow resonances can form around the eigenenergy values in the corresponding closed system. When some variations to the dot geometry are introduced so that the underlying classical dynamics becomes fully chaotic, no stable periodic orbits can exist. While scars can still be formed around these orbits in the closed system,⁷ the corresponding resonant states in the open system generally will have much shorter lifetimes, effectively eliminating the narrow resonances in conductance fluctuations. Since the system is open, chaos is transient, which is supported by a non-attracting chaotic set in the phase space.⁸ If the intrinsic characteristics of the set can be adjusted in an experimentally feasible way, the corresponding quantum conductance fluctuations may be modulated.

Our idea is to generate a region around the center of the nanostructure with high potential so that it prohibits classical particles from entering. Consider a rectangular QD, a prototypical model in semiconductor-based, two-dimensional electron gas (2DEG) systems. The classical dynamics is integrable so that extremely narrow resonances can arise in the quantum transport dynamics of the open-dot system. Now imagine applying a gate voltage to generate a circular, classically forbidden region around the center of the dot, which we call *black region* [Fig. 1(a)]. Classically, the closed system is thus a Sinai billiard, which is fully chaotic. Quantum mechanically, we thus expect to observe progressively smooth variations in the conductance with, e.g., the Fermi energy.

We use the tight-binding paradigm and the Landauer-Büttiker formalism in combination with the non-equilibrium Green's function method to calculate the transmission and the local density of states (LDS).¹ To demonstrate the working of our modulation scheme, we consider four different QD geometries: rectangular QD, rectangular QD with a rectangular black region, and Sinai QDs of radii $R = 0.14 \mu\text{m}$

^{a)} Author to whom correspondence should be addressed. Electronic mail: huangl@lzu.edu.cn.

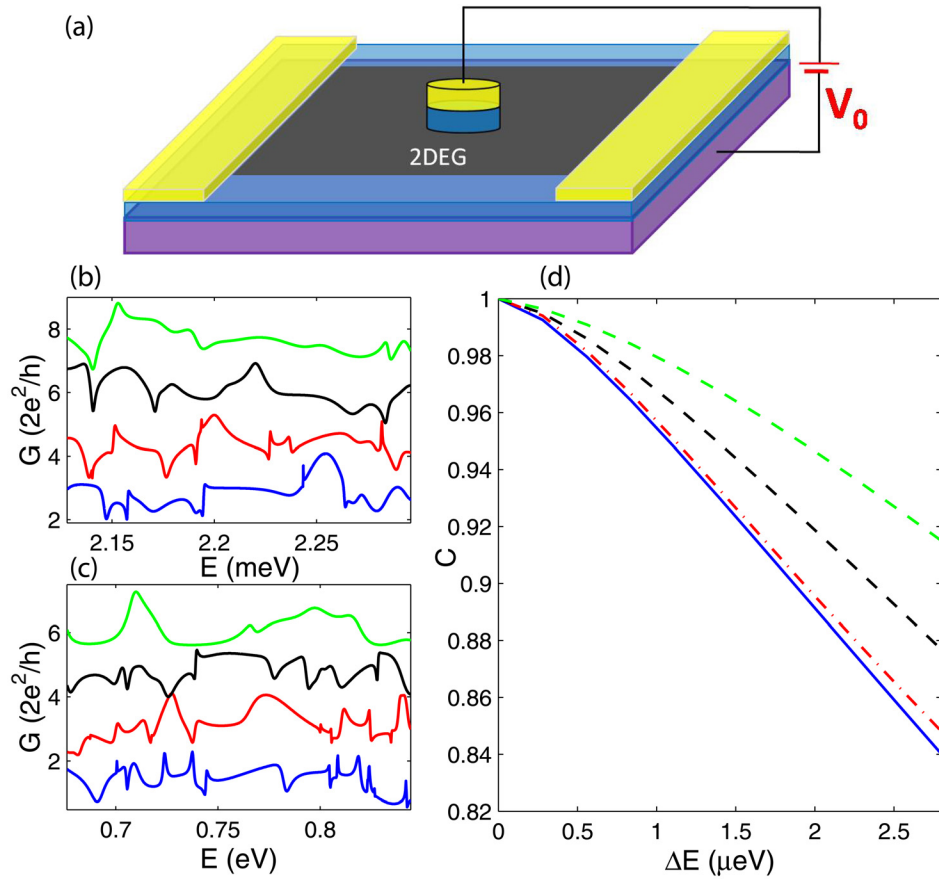


FIG. 1. (Color online) (a) Schematic of proposed experimental setup to modulate quantum transport through 2DEG formed at a GaAs/Al_{0.3}Ga_{0.7}As heterostructure, which is on n^+ Si substrate (purple/light shaded), covered by 300 nm SiO₂ (blue/dark), and contacted by Au/Cr (yellow/white). The square quantum-dot region has the side length of 1.0 μm , and the circular potential applied at the central region of the dot has a radius varying between 0.1 μm and 0.4 μm . (b) Quantum conductance versus Fermi energy for four semiconductor 2DEG QD systems (bottom to top): rectangular QD, rectangular QD with a rectangular black region of area 0.25 $\mu\text{m} \times 0.25 \mu\text{m}$, and Sinai QDs of radii $R=0.14 \mu\text{m}$ and $R=0.28 \mu\text{m}$. (c) Conductance fluctuation patterns for graphene QDs of the same geometry as in (b).⁹ (d) Autocorrelation corresponding to the four cases in (b).

and $R=0.28 \mu\text{m}$, where the classical dynamics is integrable for the first two cases and fully chaotic for the latter two cases. In all cases, we assume that the dot systems are of either semiconductor 2DEG [Fig. 1(b)] or graphene [Fig. 1(c)]. Qualitatively, we observe the appearance of sharp resonances in the transmission curves for the integrable QDs, while the curves appear smooth in the chaotic cases. This can be better seen by calculating the autocorrelation decay curves associated with the transmission fluctuation patterns [Fig. 1(d)], which decays faster for the integrable cases but slower for the chaotic cases. As the radius of the black region is increased, there is continuous improvement in the smoothness of the fluctuation patterns. These results also illustrate that generating a black region in the center of the rectangular dot is not necessarily effective in removing the narrow resonances in the quantum transmission curve (e.g., comparing the integrable cases: the two lower blue and red curves). It is *chaos* which is effective in eliminating the resonances (the two upper black and green curves). Similar behaviors have been observed for the graphene QDs [Fig. 1(c)].

To develop a physical theory to understand the mechanism of chaos-based modulation of quantum transport, we note that under the tight-binding paradigm, the QD can be regarded as a closed system of Hamiltonian matrix H_c and the leads be treated by retarded self-energy matrices Σ^R . The matrix H_c is Hermitian with a set of real eigenenergies and eigenfunctions $\{E_{0\alpha}, \psi_{0\alpha}\}$, but $\Sigma^R(E_0)$, in general, is not Hermitian and depends on the Fermi energy E_0 . The effective Hamiltonian matrix $H_c + \Sigma^R(E_0)$ thus has a set of complex eigenenergies with the eigenfunctions: $[H_c + \Sigma^R(E_0)]\psi_\alpha$

$= E_\alpha \psi_\alpha$, where $E_\alpha = E_{0\alpha} - \Delta_\alpha - i\gamma_\alpha$, Δ_α is a shift in the eigenenergy induced by Σ^R , and γ_α characterizes the energy scale of the transmission resonance caused by ψ_α .^{1,10} We then calculate the first-order approximation of $\Delta_\alpha + i\gamma_\alpha$, which is given by $\Delta_\alpha + i\gamma_\alpha \approx -\langle \psi_{0\alpha} | \Sigma^R | \psi_{0\alpha} \rangle$.¹⁰ We obtain $E_\alpha = E_{0\alpha} - \Delta_\alpha - i\gamma_\alpha \approx E_{0\alpha} + \langle \psi_{0\alpha} | \Sigma^R | \psi_{0\alpha} \rangle$ [Eq. (1)]. In general, Σ^R can be expressed as¹ $\Sigma^R = -t \sum_L \sum_{m \in L} \chi_{m,L} \exp(ik_m a) \chi_{m,L}^\dagger$, where L is the lead index and $\chi_{m,L}$ is the transverse mode m in lead L . Since Σ^R only has nonzero elements at the boundary points of the QD connecting with the leads, only the values of $\psi_{0\alpha}$ on the same set of discrete points, $\psi_{0\alpha,L}$, contribute to γ_α . Since $\{\chi_{m,L}\}$ form a complete and orthogonal basis, $\psi_{0\alpha,L}$ can be expanded as $\psi_{0\alpha,L} = \sum_m c_m \chi_{m,L}$. Substituting this into Eq. (1) and taking into account the mirror symmetry of the system, we obtain $E_\alpha \approx E_{0\alpha} - 2t \sum_m |c_m|^2 \exp(ik_m a)$ [Eq. (2)].

For validation, we consider one small rectangular QD of 0.2 $\mu\text{m} \times 0.2 \mu\text{m}$. Since Σ^R depends on E_0 , Δ_α and γ_α are also functions of E_0 . Thus, our theory is precise only for eigenstates close to E_0 .¹ In this example, we use $E_0 = 2.5293 \text{ meV}$. We observe a good correspondence of the positions of the transmission resonances and their widths to the real and imaginary parts of the eigenenergies of $H_c + \Sigma^R(E_0)$ (crosses), respectively, as shown in Fig. 2. The eigenstates whose values of γ_α are approximately 10^{-1} meV contribute to the smooth, background conductance variations. However, eigenstates whose γ_α values are in the range 10^{-3} meV to 10^{-2} meV correspond to localized states; for example, the four states indicated by the dash-dotted lines. A good agreement between theory and simulation is obtained.

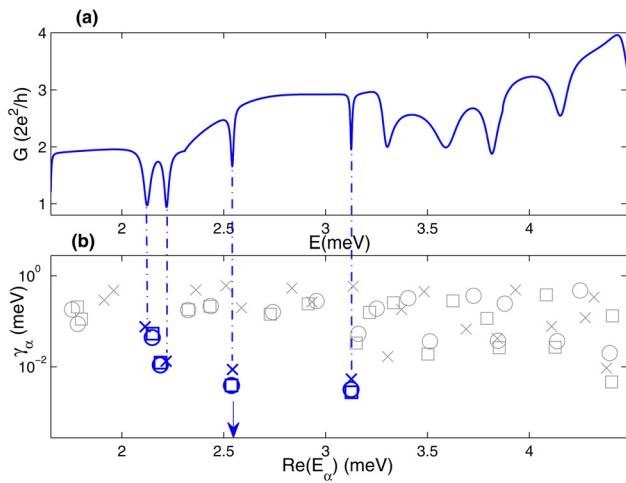


FIG. 2. (Color online) (a) Conductance versus energy for one small QD of $0.2 \mu\text{m} \times 0.2 \mu\text{m}$ (see text); (b) the corresponding real and imaginary parts of eigenenergy E_α of $H_c + \Sigma^R(E_0)$ (cross), calculated from Eq. (1) (square) and Eq. (2) (circle). The Fermi energy is $E_0 = 2.5293 \text{ meV}$, as indicated by the arrow.

Our chaos-based modulation mechanism can then be understood as follows. First, the degree of the conductance fluctuations can be inferred from the distribution of γ_α values. In particular, smaller γ_α values indicate more severe (sharper) resonances. Fig. 3 shows the distribution of γ_α in a proper energy range, where Σ^R is evaluated at $E_0 = 2.7862 \text{ meV}$. In particular, in Fig. 3(a), the values of γ_α spread out far below $5 \times 10^{-4} \text{ meV}$, even to 10^{-6} meV , which correspond to the localized states in the rectangular QD. However, for the chaotic Sinai QDs, most values of γ_α are concentrated above $5 \times 10^{-4} \text{ meV}$, as shown in Figs. 3(c) and 3(d). Note that the integrable QD with a central rectangular black region [Fig. 3(b)] has approximately the same number of eigenstates as the chaotic Sinai QD with $R = 0.14 \mu\text{m}$ [Fig. 3(c)] but the distributions of γ_α values are different for the two cases in that there are significantly more localized states in the integrable QDs. For the chaotic QD, as the radius of the central black region is increased, there is a

progressive disappearance of eigenvalues with extremely small imaginary parts and, hence, resonances of extremely narrow width, leading to more smooth fluctuation patterns. Second, since Σ^R for all the QDs considered are the same for a given energy E_0 , the difference in the values of γ_α is solely determined by the quantity c_m , which is the projection of the eigenfunction coupled to the lead, $\psi_{0\alpha,L}$, onto the transverse modes of the lead, $\chi_{m,L}$. For the integrable QDs, there are localized states corresponding to the marginally stable orbits. As a result, these states couple to the leads only weakly, leading to small c_m . For the chaotic QDs with relatively large escape rates, unstable periodic orbits dominate, so the resonant states are not as pronounced as for the regular QDs. These considerations can be demonstrated directly from the LDS patterns, as shown in Figs. 3(e)–3(h). For the integrable QDs without and with central rectangular black region [Figs. 3(e) and 3(f)], the LDS patterns associated with the resonant states are well localized, which correspond to the classical “bouncing-ball” orbits. For the chaotic Sinai QDs, the LDS patterns are strongly affected by the central circular black region, in which they appear much less localized and relatively more uniform than those in the integrable QDs, which results in a strong coupling to the leads.

In summary, we have proposed and validated a scheme of quantum modulation based on classical transient chaos. The key physics underlying our method is that chaos in the classical limit has a profound effect on the resonant or pointer states in the corresponding quantum transport system. We have provided a self-consistent theoretical argument to fully explain our chaos-based modulation scheme, with strong numerical support (Fig. 3) (in contrast, in our recent work,¹⁰ we focused on Fano-resonance formula and the comparison of features of scarring between non-relativistic quantum and graphene systems). The chaos-based quantum modulation scheme is conceptually appealing and experimentally feasible, and further interest and effort are warranted to explore this idea for significant applications in nanoscience and nanotechnology.

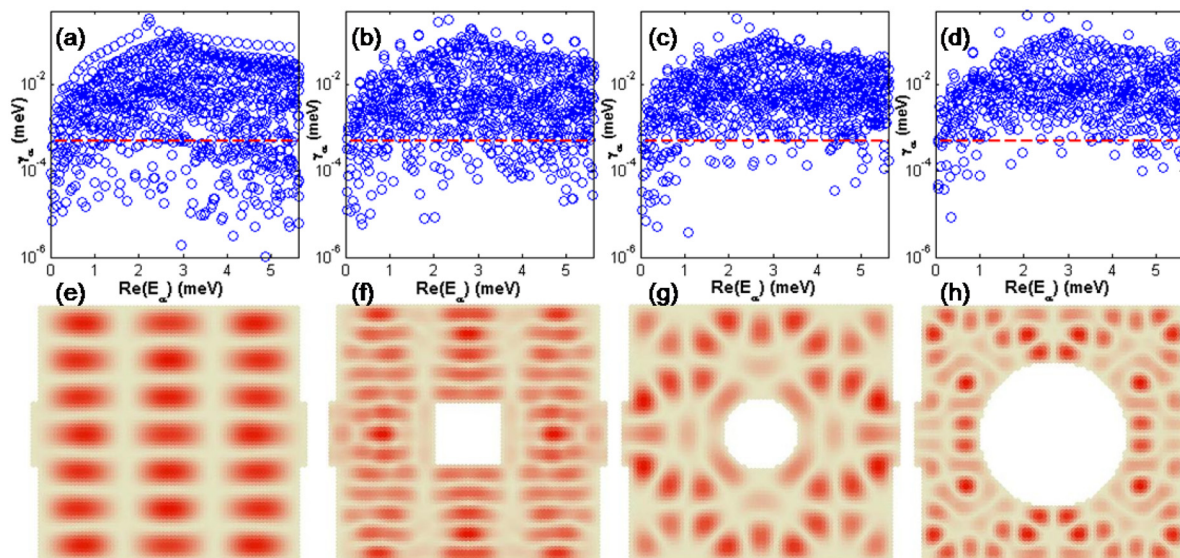


FIG. 3. (Color online) Real and imaginary parts of the eigenenergies E_α for (a) rectangular QD, (b) QD with a rectangular black region, (c) Sinai QD with $R = 0.14 \mu\text{m}$, and (d) Sinai QD with $R = 0.28 \mu\text{m}$, where $E_0 = 2.7862 \text{ meV}$ for all cases. The eye-guiding dashed lines indicate $\gamma_\alpha = 5 \times 10^{-4} \text{ meV}$. (e)–(h) Typical quantum pointer states for different QDs, where Fermi energies (meV) are 0.3213, 0.9668, 0.5522, and 1.1680, respectively.

This work was supported by AFOSR under Grant No. FA9550-09-1-0260 and by ONR under Grant No. N00014-08-1-0627. L.H. was also supported by NSFC under Grant No. 11005053.

- ¹S. Datta, *Electronic Transport in Mesoscopic Systems* (Cambridge University Press, Cambridge, UK, 1995).
- ²R. A. Jalabert, H. U. Baranger, and A. D. Stone, *Phys. Rev. Lett.* **65**, 2442 (1990); R. Ketzmerick, *Phys. Rev. B* **54**, 10841 (1996); R. P. Taylor, R. Newbury, A. S. Sachrajda, Y. Feng, P. T. Coleridge, C. Dettmann, N. Zhu, H.-G. A. Delage, P. J. Kelly, and Z. Wasilewski, *Phys. Rev. Lett.* **78**, 1952 (1997); G. Casati, I. Guarneri, and G. Maspero, *Phys. Rev. Lett.* **84**, 63 (2000); R. Crook, C. G. Smith, A. C. Graham, I. Farrer, H. E. Beere, and D. A. Ritchie, *Phys. Rev. Lett.* **91**, 246803 (2003).
- ³A. H. Castro Neto, F. Guinea, N. M. R. Peres, K. S. Novoselov, and A. K. Geim, *Rev. Mod. Phys.* **81**, 109 (2009).
- ⁴E. Ott, C. Grebogi, and J. A. Yorke, *Phys. Rev. Lett.* **64**, 1196 (1990).
- ⁵L. M. Pecora, H. Lee, D.-H. Wu, T. Antonsen, M.-J. Lee, and E. Ott, *Phys. Rev. E* **83**, 065201 (2011).
- ⁶W. H. Zurek, *Rev. Mod. Phys.* **75**, 715 (2003); D. K. Ferry, R. Akis, and J. P. Bird, *Phys. Rev. Lett.* **93**, 026803 (2004).
- ⁷S. W. McDonald and A. N. Kaufman, *Phys. Rev. Lett.* **42**, 1189 (1979); E. J. Heller, *Phys. Rev. Lett.* **53**, 1515 (1984); E. B. Bogomolny, *Physica D* **31**, 169 (1988); M. V. Berry, *Proc. R. Soc. London, Ser. A* **423**, 219 (1989); L. Huang, Y.-C. Lai, D. K. Ferry, S. M. Goodnick, and R. Akis, *Phys. Rev. Lett.* **103**, 054101 (2009).
- ⁸Y.-C. Lai and T. Tél, *Transient Chaos* (Springer, New York, 2011).
- ⁹The graphene QD is 15 nm × 15 nm with about 8000 atoms. For both Figs. 1(b) and 1(c), the energy ranges when normalized by the hopping energy t are the same, $\Delta E/t = 0.06$.
- ¹⁰R. Yang, L. Huang, Y.-C. Lai, and C. Grebogi, *Europhys. Lett.* **94**, 40004 (2011).